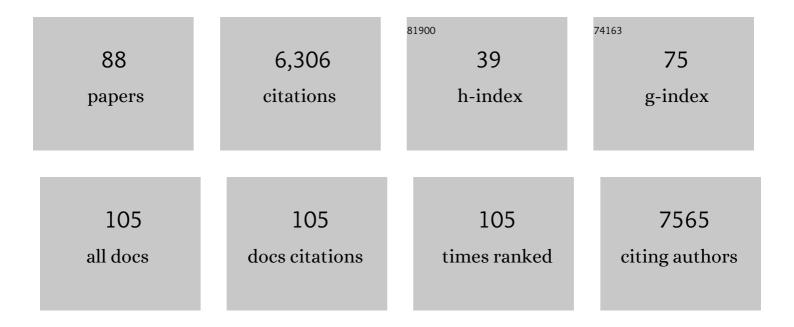
List of Publications by Year in descending order

Source: https://exaly.com/author-pdf/8820781/publications.pdf Version: 2024-02-01



CONCLU

#	Article	IF	CITATIONS
1	Atomic View of a Toxic Amyloid Small Oligomer. Science, 2012, 335, 1228-1231.	12.6	518
2	Amyloid fibril structure of α-synuclein determined by cryo-electron microscopy. Cell Research, 2018, 28, 897-903.	12.0	339
3	Selective Surface Enhanced Raman Scattering for Quantitative Detection of Lung Cancer Biomarkers in Superparticle@MOF Structure. Advanced Materials, 2018, 30, 1702275.	21.0	301
4	Toxic fibrillar oligomers of amyloid-l ² have cross-l ² structure. Proceedings of the National Academy of Sciences of the United States of America, 2012, 109, 7717-7722.	7.1	286
5	Amyloid β-sheet mimics that antagonize protein aggregation and reduce amyloid toxicity. Nature Chemistry, 2012, 4, 927-933.	13.6	213
6	Atomic structures of FUS LC domain segments reveal bases for reversible amyloid fibril formation. Nature Structural and Molecular Biology, 2018, 25, 341-346.	8.2	185
7	Out-of-register Î ² -sheets suggest a pathway to toxic amyloid aggregates. Proceedings of the National Academy of Sciences of the United States of America, 2012, 109, 20913-20918.	7.1	184
8	The structured core domain of αB-crystallin can prevent amyloid fibrillation and associated toxicity. Proceedings of the National Academy of Sciences of the United States of America, 2014, 111, E1562-70.	7.1	181
9	PARylation regulates stress granule dynamics, phase separation, and neurotoxicity of disease-related RNA-binding proteins. Cell Research, 2019, 29, 233-247.	12.0	175
10	Liquid-liquid phase separation in biology: mechanisms, physiological functions and human diseases. Science China Life Sciences, 2020, 63, 953-985.	4.9	164
11	Structural basis for reversible amyloids of hnRNPA1 elucidates their role in stress granule assembly. Nature Communications, 2019, 10, 2006.	12.8	157
12	Understanding the Selective Detection of Fe ³⁺ Based on Graphene Quantum Dots as Fluorescent Probes: The <i>K</i> _{sp} of a Metal Hydroxide-Assisted Mechanism. Analytical Chemistry, 2017, 89, 12054-12058.	6.5	143
13	Tunable assembly of amyloid-forming peptides into nanosheets as a retrovirus carrier. Proceedings of the United States of America, 2015, 112, 2996-3001.	7.1	123
14	Phase Separation of Disease-Associated SHP2 Mutants Underlies MAPK Hyperactivation. Cell, 2020, 183, 490-502.e18.	28.9	123
15	Stress Induces Dynamic, Cytotoxicity-Antagonizing TDP-43 Nuclear Bodies via Paraspeckle LncRNA NEAT1-Mediated Liquid-Liquid Phase Separation. Molecular Cell, 2020, 79, 443-458.e7.	9.7	118
16	Hsp27 chaperones FUS phase separation under the modulation of stress-induced phosphorylation. Nature Structural and Molecular Biology, 2020, 27, 363-372.	8.2	117
17	Macrocyclic β-Sheet Peptides That Inhibit the Aggregation of a Tau-Protein-Derived Hexapeptide. Journal of the American Chemical Society, 2011, 133, 3144-3157.	13.7	114
18	Parkinson's disease-related phosphorylation at Tyr39 rearranges α-synuclein amyloid fibril structure revealed by cryo-EM. Proceedings of the National Academy of Sciences of the United States of America, 2020, 117, 20305-20315.	7.1	113

#	Article	IF	CITATIONS
19	Cryo-EM structure of an amyloid fibril formed by full-length human prion protein. Nature Structural and Molecular Biology, 2020, 27, 598-602.	8.2	112
20	β2-microglobulin forms three-dimensional domain-swapped amyloid fibrils with disulfide linkages. Nature Structural and Molecular Biology, 2011, 18, 49-55.	8.2	105
21	Structure-Based Design of Functional Amyloid Materials. Journal of the American Chemical Society, 2014, 136, 18044-18051.	13.7	102
22	Cryo-EM structure of full-length α-synuclein amyloid fibril with Parkinson's disease familial A53T mutation. Cell Research, 2020, 30, 360-362.	12.0	94
23	Structure-based discovery of fiber-binding compounds that reduce the cytotoxicity of amyloid beta. ELife, 2013, 2, e00857.	6.0	94
24	Designed amyloid fibers as materials for selective carbon dioxide capture. Proceedings of the National Academy of Sciences of the United States of America, 2014, 111, 191-196.	7.1	93
25	General Strategy to Optimize Gas Evolution Reaction via Assembled Striped-Pattern Superlattices. Journal of the American Chemical Society, 2020, 142, 1857-1863.	13.7	93
26	Versatile Structures of α-Synuclein. Frontiers in Molecular Neuroscience, 2016, 9, 48.	2.9	92
27	Coordination mode engineering in stacked-nanosheet metal–organic frameworks to enhance catalytic reactivity and structural robustness. Nature Communications, 2019, 10, 2779.	12.8	89
28	Precise and Reversible Protein-Microtubule-Like Structure with Helicity Driven by Dual Supramolecular Interactions. Journal of the American Chemical Society, 2016, 138, 1932-1937.	13.7	85
29	Allosteric Inhibitors of SHP2 with Therapeutic Potential for Cancer Treatment. Journal of Medicinal Chemistry, 2017, 60, 10205-10219.	6.4	85
30	Characteristics of Amyloid-Related Oligomers Revealed by Crystal Structures of Macrocyclic β-Sheet Mimics. Journal of the American Chemical Society, 2011, 133, 6736-6744.	13.7	84
31	Parkinson's disease associated mutation E46K of α-synuclein triggers the formation of a distinct fibril structure. Nature Communications, 2020, 11, 2643.	12.8	76
32	Structural Insights into Aβ42 Oligomers Using Site-directed Spin Labeling. Journal of Biological Chemistry, 2013, 288, 18673-18683.	3.4	70
33	Hsp40 proteins phase separate to chaperone the assembly and maintenance of membraneless organelles. Proceedings of the National Academy of Sciences of the United States of America, 2020, 117, 31123-31133.	7.1	66
34	Hierarchical chemical determination of amyloid polymorphs in neurodegenerative disease. Nature Chemical Biology, 2021, 17, 237-245.	8.0	66
35	Exploiting mammalian low-complexity domains for liquid-liquid phase separation–driven underwater adhesive coatings. Science Advances, 2019, 5, eaax3155.	10.3	62
36	Antiparallel Triple-strand Architecture for Prefibrillar Aβ42 Oligomers. Journal of Biological Chemistry, 2014, 289, 27300-27313.	3.4	60

#	Article	IF	CITATIONS
37	Mechanistic basis for receptor-mediated pathological α-synuclein fibril cell-to-cell transmission in Parkinson's disease. Proceedings of the National Academy of Sciences of the United States of America, 2021, 118, .	7.1	59
38	A stable lead halide perovskite nanocrystals protected by PMMA. Science China Materials, 2018, 61, 363-370.	6.3	55
39	N-Terminal Acetylation Preserves α-Synuclein from Oligomerization by Blocking Intermolecular Hydrogen Bonds. ACS Chemical Neuroscience, 2017, 8, 2145-2151.	3.5	52
40	Liquid-liquid phase separation of RBGD2/4 is required for heat stress resistance in Arabidopsis. Developmental Cell, 2022, 57, 583-597.e6.	7.0	45
41	Conformational strains of pathogenic amyloid proteins in neurodegenerative diseases. Nature Reviews Neuroscience, 2022, 23, 523-534.	10.2	43
42	Diverse Supramolecular Nanofiber Networks Assembled by Functional Low-Complexity Domains. ACS Nano, 2017, 11, 6985-6995.	14.6	41
43	Mechanistic insights into the switch of αB-crystallin chaperone activity and self-multimerization. Journal of Biological Chemistry, 2018, 293, 14880-14890.	3.4	41
44	Sc(OTf) ₃ -Catalyzed Transfer Diazenylation of 1,3-Dicarbonyls with Triazenes via N–N Bond Cleavage. Organic Letters, 2014, 16, 5458-5461.	4.6	37
45	Structural basis of the interplay between α-synuclein and Tau in regulating pathological amyloid aggregation. Journal of Biological Chemistry, 2020, 295, 7470-7480.	3.4	34
46	The nuclear localization sequence mediates hnRNPA1 amyloid fibril formation revealed by cryoEM structure. Nature Communications, 2020, 11, 6349.	12.8	33
47	The hereditary mutation G51D unlocks a distinct fibril strain transmissible to wild-type α-synuclein. Nature Communications, 2021, 12, 6252.	12.8	33
48	Ordered Superparticles with an Enhanced Photoelectric Effect by Subâ€Nanometer Interparticle Distance. Advanced Functional Materials, 2017, 27, 1701982.	14.9	32
49	New insights of poly(ADP-ribosylation) in neurodegenerative diseases: A focus on protein phase separation and pathologic aggregation. Biochemical Pharmacology, 2019, 167, 58-63.	4.4	32
50	Structural Diversity of Amyloid Fibrils and Advances in Their Structure Determination. Biochemistry, 2020, 59, 639-646.	2.5	32
51	Different regions of synaptic vesicle membrane regulate VAMP2 conformation for the SNARE assembly. Nature Communications, 2020, 11, 1531.	12.8	30
52	Hsp70 chaperones TDP-43 in dynamic, liquid-like phase and prevents it from amyloid aggregation. Cell Research, 2021, 31, 1024-1027.	12.0	30
53	Heat shock protein 104 (HSP104) chaperones soluble Tau via a mechanism distinct from its disaggregase activity. Journal of Biological Chemistry, 2019, 294, 4956-4965.	3.4	28
54	Genetic prion disease–related mutation E196K displays a novel amyloid fibril structure revealed by cryo-EM. Science Advances, 2021, 7, eabg9676.	10.3	28

#	Article	IF	CITATIONS
55	The structure of a minimum amyloid fibril core formed by necroptosis-mediating RHIM of human RIPK3. Proceedings of the National Academy of Sciences of the United States of America, 2021, 118, .	7.1	27
56	Fibril Self-Assembly of Amyloid–Spider Silk Block Polypeptides. Biomacromolecules, 2019, 20, 2015-2023.	5.4	24
57	Wild-type α-synuclein inherits the structure and exacerbated neuropathology of E46K mutant fibril strain by cross-seeding. Proceedings of the National Academy of Sciences of the United States of America, 2021, 118, .	7.1	24
58	Programming Conventional Electron Microscopes for Solving Ultrahigh-Resolution Structures of Small and Macro-Molecules. Analytical Chemistry, 2019, 91, 10996-11003.	6.5	23
59	Mechanical penetration of β-lactam–resistant Gram-negative bacteria by programmable nanowires. Science Advances, 2020, 6, .	10.3	23
60	Generic amyloid fibrillation of TMEM106B in patient with Parkinson's disease dementia and normal elders. Cell Research, 2022, 32, 585-588.	12.0	23
61	In-Cell NMR Study of Tau and MARK2 Phosphorylated Tau. International Journal of Molecular Sciences, 2019, 20, 90.	4.1	22
62	O-Glycosylation Induces Amyloid-Î ² To Form New Fibril Polymorphs Vulnerable for Degradation. Journal of the American Chemical Society, 2021, 143, 20216-20223.	13.7	22
63	Second messenger Ap4A polymerizes target protein HINT1 to transduce signals in FcεRI-activated mast cells. Nature Communications, 2019, 10, 4664.	12.8	19
64	A Metastable Crystalline Phase in Twoâ€Dimensional Metallic Oxide Nanoplates. Angewandte Chemie - International Edition, 2019, 58, 2055-2059.	13.8	19
65	Molecular structure of an amyloid fibril formed by FUS low-complexity domain. IScience, 2022, 25, 103701.	4.1	19
66	Modular genetic design of multi-domain functional amyloids: insights into self-assembly and functional properties. Chemical Science, 2019, 10, 4004-4014.	7.4	18
67	Detecting Singleâ€Molecule Dynamics on Lipid Membranes with Quenchersâ€inâ€aâ€Liposome FRET. Angewandte Chemie - International Edition, 2019, 58, 5577-5581.	13.8	18
68	A novel partially open state of SHP2 points to a "multiple gear―regulation mechanism. Journal of Biological Chemistry, 2021, 296, 100538.	3.4	18
69	Nicotinamide mononucleotide adenylyltransferase uses its NAD+ substrate-binding site to chaperone phosphorylated Tau. ELife, 2020, 9, .	6.0	18
70	Continuous in situ portable SERS analysis of pollutants in water and air by a highly sensitive gold nanoparticle-decorated PVDF substrate. Analytical and Bioanalytical Chemistry, 2021, 413, 5469-5482.	3.7	17
71	Ultrasensitive SERS Analysis of Liquid and Gaseous Putrescine and Cadaverine by a 3D-Rosettelike Nanostructure-Decorated Flexible Porous Substrate. Analytical Chemistry, 2022, 94, 5273-5283.	6.5	17
72	Unraveling the Potential-Dependent Volcanic Selectivity Changes of an Atomically Dispersed Ni Catalyst During CO ₂ Reduction. ACS Catalysis, 2022, 12, 8676-8686.	11.2	16

#	Article	lF	CITATIONS
73	Spatiotemporal dynamic regulation of membraneless organelles by chaperone networks. Trends in Cell Biology, 2022, 32, 1-3.	7.9	15
74	A Structural View of αB-crystallin Assembly and Amyloid Aggregation. Protein and Peptide Letters, 2017, 24, 315-321.	0.9	15
75	SARS-CoV-2 impairs the disassembly of stress granules and promotes ALS-associated amyloid aggregation. Protein and Cell, 2022, 13, 602-614.	11.0	15
76	Hsp70 exhibits a liquid-liquid phase separation ability and chaperones condensed FUS against amyloid aggregation. IScience, 2022, 25, 104356.	4.1	14
77	Cryo-EM structure of an amyloid fibril formed by full-length human SOD1 reveals its conformational conversion. Nature Communications, 2022, 13, .	12.8	12
78	Proximal Single-Stranded RNA Destabilizes Human Telomerase RNA G-Quadruplex and Induces Its Distinct Conformers. Journal of Physical Chemistry Letters, 2021, 12, 3361-3366.	4.6	9
79	Detecting Singleâ€Molecule Dynamics on Lipid Membranes with Quenchersâ€inâ€aâ€Liposome FRET. Angewandte Chemie, 2019, 131, 5633-5637.	2.0	8
80	One-Step Generation and Purification of Cell-Encapsulated Hydrogel Microsphere With an Easily Assembled Microfluidic Device. Frontiers in Bioengineering and Biotechnology, 2021, 9, 816089.	4.1	8
81	Identifying Heterozipper β-Sheet in Twisted Amyloid Aggregation. Nano Letters, 2022, 22, 3707-3712.	9.1	8
82	Better Together: A Hybrid Amyloid Signals Necroptosis. Cell, 2018, 173, 1068-1070.	28.9	7
83	A Metastable Crystalline Phase in Twoâ€Dimensional Metallic Oxide Nanoplates. Angewandte Chemie, 2019, 131, 2077-2081.	2.0	7
84	Structural Insights of Fe3+ Induced α-synuclein Fibrillation in Parkinson's Disease. Journal of Molecular Biology, 2023, 435, 167680.	4.2	7
85	A high-throughput method for exploring the parameter space of protein liquid-liquid phase separation. Cell Reports Physical Science, 2022, 3, 100764.	5.6	5
86	Microfluidic disk for the determination of human blood types. Microsystem Technologies, 2017, 23, 5645-5651.	2.0	4
87	Low Cost, Easily-Assembled Centrifugal Buoyancy-Based Emulsification and Digital PCR. Micromachines, 2022, 13, 171.	2.9	3
88	The mouse nicotinamide mononucleotide adenylyltransferase chaperones diverse pathological amyloid client proteins. Journal of Biological Chemistry, 2022, 298, 101912.	3.4	1